Volume 1 | Number 1 | Jan 2013 | Pages 1–100

PCCP

Physical Chemistry Chemical Physics
www.rsc.org/pccp

ROYAL SOCIETY OF CHEMISTRY

ROYAL SOCIETY OF CHEMISTRY

www.rsc.org/pccp

Molecular structure and dynamics of aqueous sodium chloride solution in nano-pore between portlandite surfaces: a molecular dynamics study

Hou, Dongshuai[a]; Lu, Zeyu[b]; Zhang, Peng[c]; Ding, Qingjun[d]

a. **Corresponding author, Associate Professor, Qingdao Technological University, Qingdao, China, email: dhou@ust.hk;**

b. **Corresponding author, Doctor, Hong Kong University of Science and Technology, Clear Water Bay, Hong Kong, email: zluaa@ust.hk**

c. **Associate Professor, Qingdao Technological University, Qingdao, China, email: zhp0221@163.com**

d. **Professor, Wuhan University of Technology, dingqj@whut.edu.cn**

Abstract

Portlandite plays an important role in the hydration phase of the cement-based materials and influences the strength and durability of the material. This paper describes a molecular dynamics study of the structure and dynamics of water and ions confined at ambient temperature in calcium hydroxyl nanopores of width 35 Å. Strong layering of water in the vicinity of the (001) surface of portlandite demonstrates special structural features such as large density, good orientation preference, ordered interfacial organization and low diffusion rate. Due to the fixed vibration and rotation of the hydroxyl groups at the interface, water molecules within the first adsorbed layer adopt both H-downward and H-upward orientations by donating H-bonds and accepting H-bonds from the OH bonds in the solid surface. In

respect of the ions and portlandite interaction, the Na$^+$ ions, deeply rooted in spaces of the surficial hydroxyl groups, are significantly slowed down and remain near the surface for a long time. On the other hand, due to the weak H-bonds formed by chloride ions and hydroxyl adsorbed chloride ions near the surface cannot remain for longer time. In addition, when the water and ions are confined in the nano-pores, the residence time for the ions-water, ions-ions cluster is lengthened so that the ions adsorption capability for the porlandite surface is enhanced due to the stable Na-Cl connections in the electrolyte solution.

1. Introduction

As the ubiquitously utilized construction and building material, concrete inevitably suffers from the mechanical loading and chemical, physical and biological attack from the surrounding environment. This results in degradation of the performance of concrete and may result in the severe damage of the structure. Most of the durability problems of cement-based materials are closely related to the motion and transport of water and ions in these materials. For example, in the porous structure of reinforced concrete, water molecules carry detrimental ions, such as sulfate or chloride species, that are transported to the surface of the steel by capillary adsorption or diffusion, the passivation film is destroyed , accelerating corrosion of the steel. The interaction of ionic species and water molecules with the surfaces of calcium silicate hydrate and portlandite, which are mainly hydration products, is central to understanding the chemical and physical behavior of the concrete-water interface. Therefore, it is particularly important to elucidate the transport mechanism of water and ionic species through the portlandite crystal. However, the presence of a solid surface significantly influences the ionic mobility, especially in porous media such as calcium silicate hydrate, where geometrical ultra-confinement is reinforced by the interactions between the ionic species and the disordered and charged channels. Many traditional methods, based on the Fick's Law, are not suitable for diffusion investigation at the molecular level. This is because the water molecules confined in the nanopores or in the presence of solid surface dramatically demonstrate different dynamic behavior compared with those in bulk solution and, in particular, exhibit a

glassy nature as a super-cooled liquid (Youssef, et al., 2011).

Water transport and chloride diffusion behavior in cement-based materials have been widely investigated by pore solution expression, leaching experiments, sorption isotherm measurements, and direct EDAX analyses (Castellote, et al., 1999) (Delagrave, et al., 1998). Most of these experiments involved modifying the physical and chemical environments of the solid/solution and hence reduced the accuracy in the investigation. To better quantitatively describe the sorption of chloride ions near the portlandite surface, ^{35}Cl NMR relaxation methods (Yu & Kirkpatrick, 2001) and a two-site exchange model have been proposed to study the in situ molecular-scale structural and dynamical properties of the chloride binding on the $Ca(OH)_2$ in contact with the aqueous chloride solution. Furthermore, the structural and dynamic properties of the water molecules in cement-based materials, including the interlayer water, surface water and water in the capillary pores, have been probed by ^{1}H nuclear magnetic resonance (H NMR) (Greener, et al., 2000), quasi-elastic neutron scattering (QENS) (Bordallo, et al., 2006) and the proton field cycling relaxometry approach (PFCR) (Korb, et al., 2007). These experimental results suggest that the mobility of water molecules in cement-based materials is significantly dependent on the local chemical environment. For instance, unbound water molecules in the pores move at a fast rate (diffusion coefficient~ 10^{-9} m^2/s), while the water molecules confined in the gel pores diffuse slowly (~10^{-10} m^2/s) (Bordallo, et al., 2006).

However, investigating the water structure and dynamics by experimentation alone is challenging, due to certain limitations, such as the material purity and the measurement accuracy at the relevant lengths and timescales. Computational methods can help to interpret the experimental results and play a complementary role in understanding the structural and dynamic properties at the molecular level. Molecular dynamics (MD) is a computational method that can give a more quantitative illustration of the structure, dynamics and energy of solid-liquid interfaces. Kalinichev (2007) (Kalinichev, et al., 2007), whose group developed the ClayFF force field (Cygan, et al., 2004) , introduced the force field model in a cement system and

investigated the multi-phases in the cement based material. In light of the mineral interface properties, MD simulation was performed to study the water confined between the brucite layers (Wang, et al., 2004). In addition to the water/cement interface study, they also performed MD simulation to investigate the structure and dynamic behavior of chloride at the interface between the cement hydrate and the ions solution (Kalinichev & Kirkpatrick, 2002). Because the ClayFF force field can characterize the molecular structure and dynamics properties of various phases in cement hydrate, it is suitable in simulating the cement-based material at nano-level. In the respect of computational algorithm, for the large scale and longtime statistical molecular simulation, a model for including electric fields in molecular dynamics has been developed by using an atomistic-to-continuum framework (Templeton, et al., 2011). The method has been employed to simulate salt water transport in slab-like geometries to achieve computational efficiency. Hence, this long-range electric field solver might play important role in bridging transport simulation between the atomistic level and micro-level.

In this paper, molecular dynamics is utilized to simulate water and ions transportation in the nano-pores confined by portlandite crystals. The simulation aims at giving insights on the molecular structure, dynamic motion and interaction between water and the portlandite surfaces. Density profiles, atomic trajectories, diffusion coefficients, pair correlated function and H-bond networks are used to characterize the structural and dynamic behavior of the water molecules in the nano-pores. In addition, Cl^- and associated cations diffusion are also investigated to determine the chemical and physical reactivity between portlandite surface and ions.

2. Methodology

2.1 Model Construction

The layered structures of calcium hydroxide are constructed by the calcium octahedrons with calcium atom in the center. Between the calcium layers there are

hydroxyl groups, the H-bonds of which play a role in layer connection. As shown in Fig.1a, the calcium hydroxide is cleaved in the [0 0 1] direction and the hydroxyl groups are left on the surface. Previous research has demonstrated that the first layer of water near the surface is greatly influenced by hydroxyl groups from the hydrophilic substrate, such as brucite or gibbsite surface (Wang, et al., 2004). As shown in Fig. 1b, 1200 water molecules are inserted into the narrow space between the portlandite substrate to simulate water transport confined in a 35 Å crack. In this simulation, the Ca-O-H angle constraint in ClayFF force field, which is an optional part, is not fixed in the simulation. This results in more flexible vibration of the surface hydroxyl and characterizes interactions from the neighboring surface water.
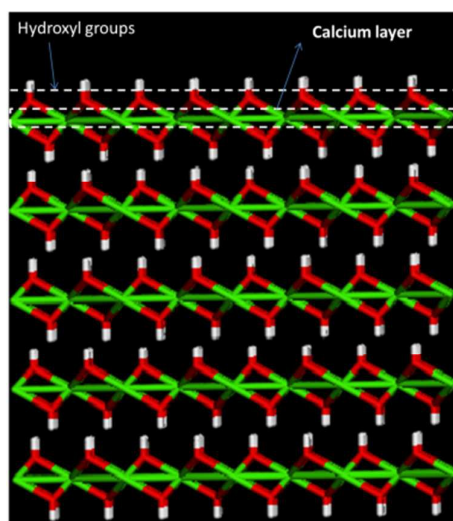
(a)
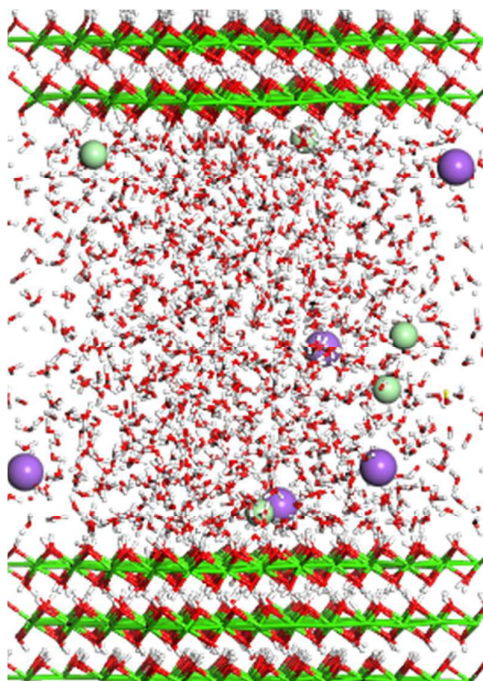
(b)

Fig.1 (a) Cleaved structure of calcium hydroxide. (b) Ca(OH)$_2$ and NaCl solution interface. Green sticks represent the calcium layers and red and white sticks are the hydroxyl groups, light green sphere is a Cl ion and the purple one is Na ion.

2.2 Force field and Molecular dynamics algorithm

In this simulation, the ClayFF force field (Cygan, et al., 2004) was employed to describe the aqueous cation, water solution and portlandite. Due to the good transferability and reliability, the ClayFF force field has already been used to successfully model the structures of oxide and hydroxide materials, the interactions of aqueous species with oxide and hydroxide surfaces, and the behavior of water and ionic species in the interlayers of layer-structure phases (Kirkpatrick, et al., 2005) (Kirkpatrick, et al., 2005) (Cygan, et al., 2009). The molecular structure and mechanical properties of portlandite were first simulated by using the ClayFF force field. As shown in Table.1, the computed structure of portlandite matches well with the experimental results (Desgranges, et al., 1993) (Holuj, et al., 1985) and previous

computational results (Laugesen, 2005) including the cell parameters, chemical bonds and elastic properties.

Portlandite			
	ClayFF	**DFT[a]**	**Exp[b,c]**
a(Å)	3.567	3.609	3.589
b(Å)	3.567	3.609	3.589
c(Å)	4.908	4.864	4.911
α(deg)	90	90	90
β(deg)	90	90	90
γ(deg)	120	120	120
vol(Å3)	54.08	54.8	54.8
Ca-OH bond (Å)	2.39	2.38	2.369
K(Gpa)	33.56	31.4	39.6
G(Gpa)	12.63	18.3	13.4

Table 1: ClayFF Computed Lattice Parameters and Elastic Properties for the Studied Crystals and Their Comparison with DFT Simulations and Experimental Data

a. DFT results from reference (Laugesen, 2005)

b. structural properties from reference (Desgranges, et al., 1993)

c. mechanical properties from reference (Holuj, et al., 1985)

The total potential interaction energy of the simulated system, U, is calculated as the sum of the electrostatic term for all Coulomb interactions between partial atomic charges and the Lennard-Jones (12-6) term modeling the short-range van der Waals dispersive interactions:

$$U = \sum_{i,j} \left\{ \frac{q_i q_j}{4\pi\epsilon_0 r} + 4\epsilon_{ij} \left[\left(\frac{\sigma_{ij}}{r_{ij}}\right)^{12} + \left(\frac{\sigma_{ij}}{r_{ij}}\right)^{6} \right] \right\} \tag{1}$$

where r_{ij} is the distance between atoms i and j, q_i and q_j are partial charges centered on these atoms, σ and ϵ are parameters of the Lennard-Jones interaction potential, and ϵ_0 is the dielectric permittivity of vacuum (equal to 8.85419×10^{-12} F/m). These parameters and partial charges are listed in table 2. The Lennard-Jones parameters, a combination of different ions interaction, can be obtained as follows:

$$\sigma = \frac{\sigma_{ii} + \sigma_{jj}}{2} \tag{2}$$

$$\epsilon_{ij} = \sqrt{\epsilon_{ii}\epsilon_{jj}} \tag{3}$$

All long range electrostatic interactions are implemented by the Ewald summation method.

Species	q/e	σ/ Å	ε/kcal/mol
oxide/hydroxide structure			
O(portlandite)	-0.95	3.166	0.1554
H(hydroxyl group)	0.425	0	0
Ca(portlandite)	1.05	5.56	5.0298×10^{-6}
water and ions			
Cl$^-$	-1	4.4006	0.1
Na$^+$	1	2.35	0.1301
H(water)	0.41	0	0
O(water)	-0.82	3.166	0.1554

Table 2: ClayFF force field parameters for different atoms

MD simulation is performed by using LAMMPS software (Plimpton, et al., 2001), which has high computational efficiency for large scale system simulation. Our simulation for the transportation consists of energy minimization to eliminate configurations that have inappropriate atoms coordinates distribution. After energy minimization, the molecular dynamics was performed as the following procedure: firstly, the calcium hydroxyl substrates were "frozen" by rigid body algorithm and only water molecules and ions were relaxed for 100 ps; followed by another 300 ps MD steps for the whole system to reach thermodynamic equilibrium state ;finally 400 ps to 10000ps equilibrium stage during which the trajectories of atoms are recorded for statistical analysis. During all the periods, the NVT ensemble was employed. The

time step was set as 0.1 fs, which can describe the dynamics of H-bonds and every 100 steps, the configuration information was recorded for data analysis.

3. Results and discussion

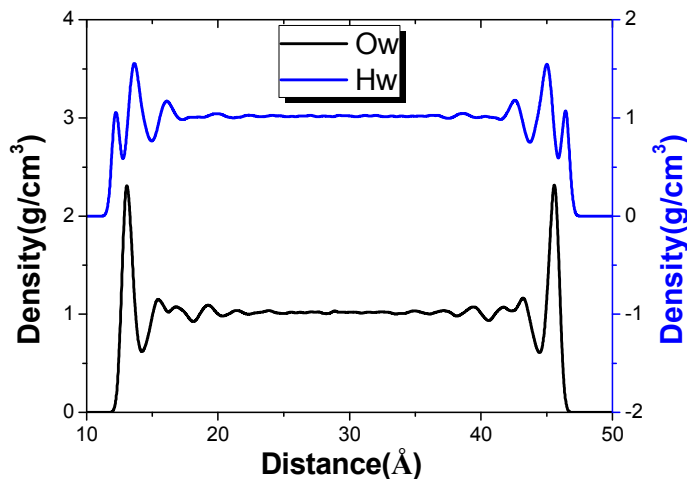### 3.1 Atomic density profile and angular distribution

Fig. 2 Density profiles for water oxygen and water hydrogen

Atomic density profiles along the direction normal to the substrate surface were calculated by averaging more than 10000 frames of MD trajectories. Atomic density oscillation with the distance from the surface on the first step provides insights into the influence of hydroxide surface on the interfacial water molecules. The surface plane is defined as the center of the interfacial hydroxyl groups (z=11.2Å). For the O_w-density profile, it can be observed in Fig. 2 that there are four obvious peaks at 13.05, 15.4, 16.9, 19.3 Å and smaller variation still exists up to 25.2 Å. For the H-density profiles, the system exhibits three obvious peaks at 12.2, 13.6, 16.1Å and few significant variations exist at 20.2 Å. The bulk water distribution is perturbed by the substrate confinement and the density profiles with different peaks are mainly the result of the substrate structure, the H-bond network of the interfacial zone as well as the local charge distribution.
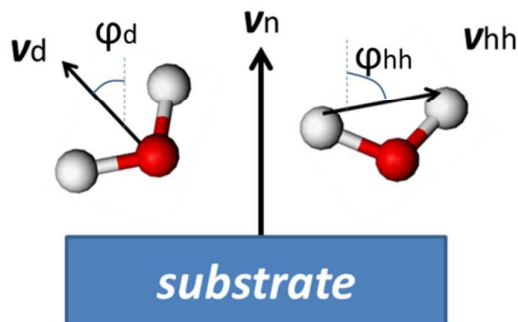
Fig.3 Water orientation: dipole angle and HH angle;

The orientation profiles, describing the water angle distribution, are defined by two specific angles: ϕ_d and ϕ_{HH}. As illustrated in Fig.3, the former is the angle between the dipole vector (v_d) of single water and the normal vector (v_n) for the surface, while the latter is the angle between v_{hh} (the vector from one H to the other in the same water) and v_n. Those instantaneous orientations of water molecules in different layers have different characteristic that can be utilized to analyze the surface influence.
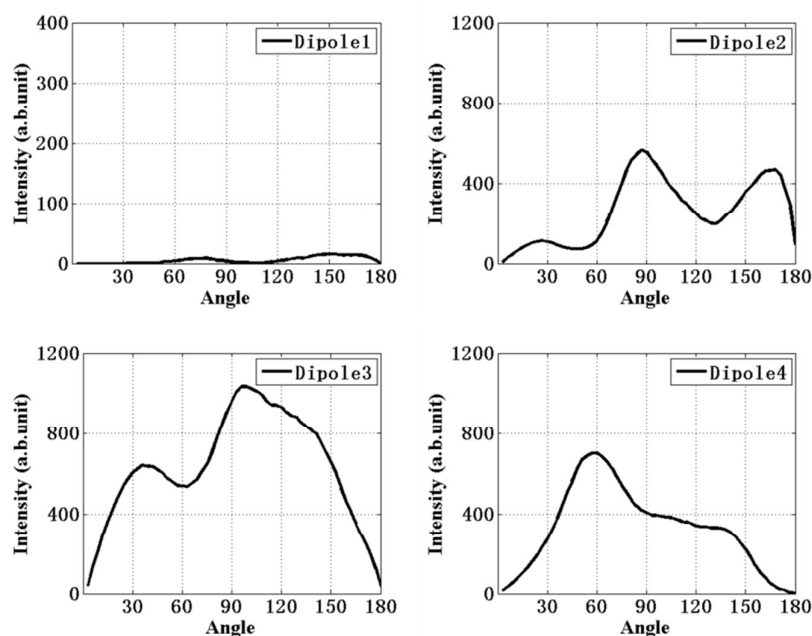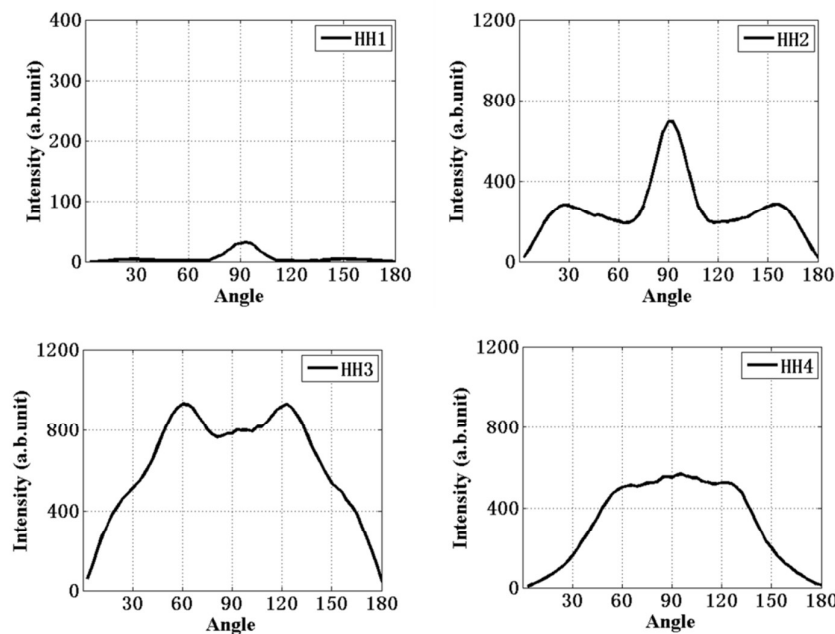
Fig.4 Orientation profiles (a) dipolar angle distribution; (b) HH angle distribution

Combined with the density profiles, the averaged orientation profiles play supplementary roles in better explaining the water structure. The dipole angle, defined as the dipole vector with [001] direction and the HH angle, the HH vector with [001] direction can provide useful information about the angle distribution. Water molecules contributing to the first density peak in the O_w profile are decomposed into 4 layers (0.5 Å for each layer). As shown in Fig. 4a, three obvious peaks can be observed in the 1st and 2nd layers (dipole 1 and 2), indicating multiple minima in the potential energy surface. On average, the dipole angles show peak values at 30°, 90°and 175°, which are defined arbitrarily as type 1, type 2 and type 3 water molecules for distinguishing in following analysis. In the lower layer (dipole 1in Fig. 4a), the water molecules orientation has two preferences from 60° to 90° and from 120° to 180°. The former orientation corresponds to water molecules with O-H vector pointing slightly upward to the surface, while the later one is contributed by those with two OH bonds pointing downward to the surface. In the layer with a mean distance 1.6 Å from the surface (dipole 2 in Fig. 4a), another small peak occurs at 30° in the dipole distribution, indicating a small percentage of water molecules with their axes tilting

upwards. In the 3rd layer, the peak intensity for type 1 water molecules increase, while the other two peaks merge together and form one large peak from 60° to 180°. The large overlapping peak is contributed by the type 2 and type 3 water molecules and also their neighbor water molecules at upper layer. Finally, water molecules in 4th layer have average dipole angle at 60°and a broad shoulder with low intensity from 90° to 140°. Previous research has focused on the interfacial water on the brucite, an Mg analogue of portlandite. The simulation results demonstrated that two types of water molecules exist on the surface: the O-H bonds of type 1 water molecules point downward with a predominately dipole angle of 130° towards surface, while the dipole vector of the type 2 water molecules points upward with an average dipole angle of 30°~80° (Wang, et al., 2004). The structural difference between Mg(OH)2 and Ca(OH)2 result in the discrepancies of the profiles of the surface water orientations. Even though the two analogues expose hydroxyl groups near the surface, portlandite has larger separation between nearest hydroxyl neighbors than that of brucite due to the larger atomic radius for the Ca atoms. Therefore, the larger cavity on the surface results in less restriction for the surface hydroxyls, which leads to a wider variation of water orientation. In Fig. 4b, a dominant orientation at 90° in the HH angle distribution provides insights that the z coordinates of two H atoms in a water molecule tend to the same height. The HH orientation is mainly attributed to type 1 water molecules with both OH bonds pointing upward and type 3 water molecules with both OH vectors pointing downward. Combined with H-bonds connection, the molecular configuration for three types of water molecule can be further discussed in Fig.8 in the following section.
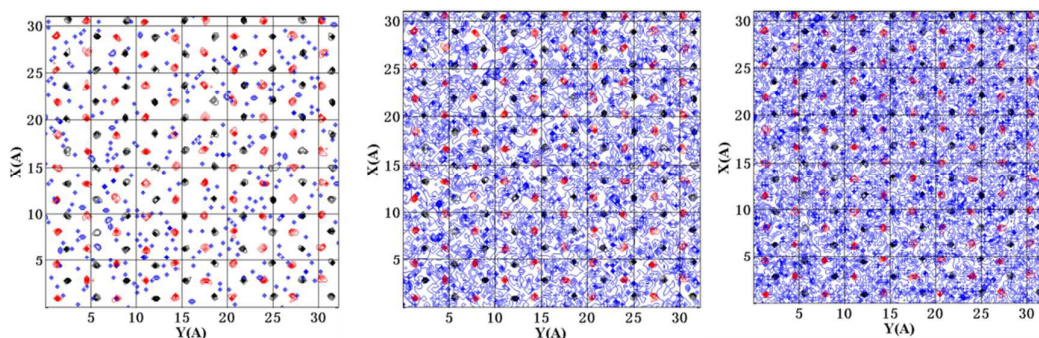
Fig. 5 Atomic density contours

Atomic maps in the 1st layer show that the water molecules occupying the cavity between neighboring hydroxyl groups are mainly from type 1 and type 3. No obviously distinguishing feature between type 1, type 2 and type 3 water molecules can be observed in the 2nd layer. Because water molecules of all types coexist in the same plane and are mixed together by the interconnected H-bonds, it is rather difficult for any type of water to aggregate in local environment. The layered surface water structure and the narrow angular orientation profiles indicate that the surface water molecules are strongly restricted by the surface hydroxyl. They are better organized and less mobile than in the bulk water solution with random distribution.
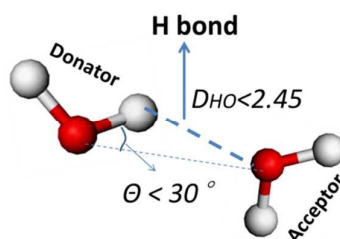
3.2 H-bonds and coordination number

Fig.6 H-bond schematic illustration. The H bond formation requires two conditions: two water neighbors distance D_{HO} should be less than 2.45 Å and the angle θ between the OH vector and the OO vector should be less than 30°. If both conditions are satisfied, the one that provides the H atoms to form H-bond is called donator while

the oxygen container is defined as the acceptor. Similarly, the substrate element can also play the role of H-bond donator or acceptor.
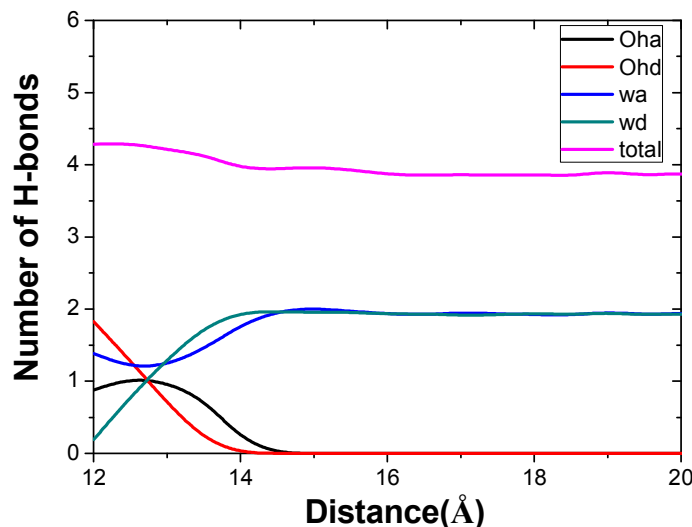

Fig.7 H bonds number evolution with distance from surface and decomposed H-bonds distribution: wa, water molecules accept H-bonds from neighboring water; wd, water molecules donate H-bonds to neighboring water; oha, water molecules accept H-bonds from surficial hydroxyl; ohd, water molecules donate H-bonds to surficial hydroxyl

The H-bond network is important in characterizing the water structures and in describing the interaction between the substrate and the neighboring water molecules. The definition of H-bond is schematically illustrated in Fig. 6. H-bond network structures are constructed by the both the contribution from the water molecules and the surface element. Therefore, to describe the local H-bond environment, it is necessary to calculate the average H-bond numbers, the average H-bond number donated and accepted by the neighboring water molecules and the substrate element.

The H-bond network in the interfacial region plays an essential role in determining the water structures, such as orientation and atomic density distribution. The number

of H-bonds decreases monotonously from 4.3 at the surface to 3.8 up to 8 Å away from surface. Differing from tobermorite and jennnite interface (Hou, et al., 2015) (Hou & Li, 2014), there is no complicated H-bonds connection with the channel element of the surface water molecules. The H-bonds connections result from interaction between calcium hydroxyl and surface water molecules. To considerable understand the H-bonds network, the bonds distribution is decomposed into four types illustrated in Fig.7. As shown in Fig.7, the number of water molecules that play the role of donators starts with a relative low value of less than 0.25, while the water acceptors contribute to nearly 1.5 H bonds. It means that the water molecules nearest to the surface predominately accept H-bonds from the up-layer water molecules. With increasing distance from the surface, the H-bonds resulting from the interconnections with the surface elements gradually decrease, while those contributed by the neighboring water molecules continuously increase.. 2.8 Å away from the surface, the water molecules no longer form H-bond connections with any surficial O. When the water molecules are 8 Å away from surface, both water acceptors and donators contribute to 1.9 H bonds, which is quite similar to the case in the bulk water solution.

The local H-bond network can also be used to interpret the angular distribution of three types of water molecules. As illustrated in Fig.8, type 3 water molecules have both H atoms donating to O in the hydroxyl; hence the dipole axes turns directly downwards. Additionally, they are likely to accept 3 H-bonds from the surrounding water molecules and another hydroxyl. Type 2 water molecules turns slightly downward and show different H-bonds connections.The water molecule donates 1 H-bond to surface O, accept 1 (or 2) H-bonds from surface H. Meanwhile it can form another 2 (or 1) H bond with neighboring water molecules. At the region about 2.5 Å from surface, water molecules with 1 or 2 H bonds donated by the surface hydroxyl tilt upwards. On average, type 1 water molecules donate less than 1 H-bond to the surface hydroxyl.
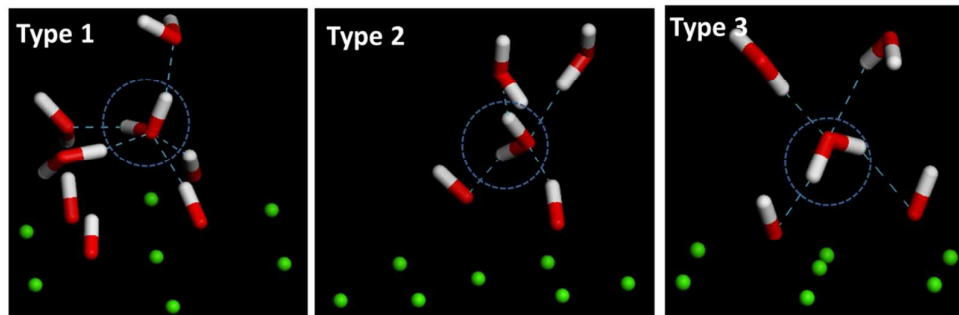
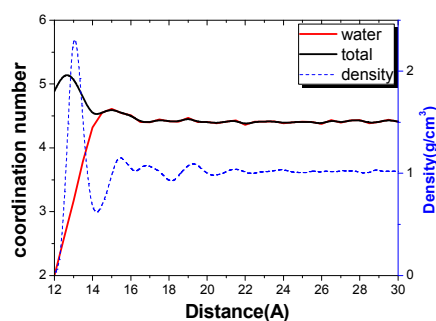Fig. 8 three types of water molecules near the calcium hydroxide surface.

Fig. 9 Coordination number of oxygen for water molecules

In addition to the H-bonds, the nearest neighbor (NN) atoms (especially oxygen atoms) play an important role in determining the local organization of the water structure. The NN number can be both contributed from the surface elements and from neighboring water molecules. As shown in Fig.9, on average, for a single water molecule, the coordination number is 4.9 at 12 Å, and reaches a peak value of 5.1 and then decreases to bulk water value 4.4. On average, more than 0.6 O atoms are not able to form H-bonds with the water molecules. The coordination oxygen, without forming H bonds with the water molecules, still plays important role in the surface network construction. For example, a type 3 water molecule can donate 2 H-bonds to the surficial oxygen, as illustrated by the case 1 in Fig.10, or it can donate 2 H-bonds to surface oxygen and accept 1 H-bond from the surface (case 2). In Fig.10, for both cases, the water molecules diffuse around the center of a triangular region enclosed by three surface hydroxyls. It should be noted that the local environment of type 3 water molecule can transfer between case 1 and case 2

due to the vibration of surficial hydroxyl groups. One H atom in hydroxyl plays the role of potential H-bond donor and it combines with another two hydroxyls to restrict the mobility, structure and the orientation of type 3 water molecules. For type 1 and type 2 water molecules, there also exists potential H bonds donor or acceptor that is likely to construct H-bonds network after similar transformation.
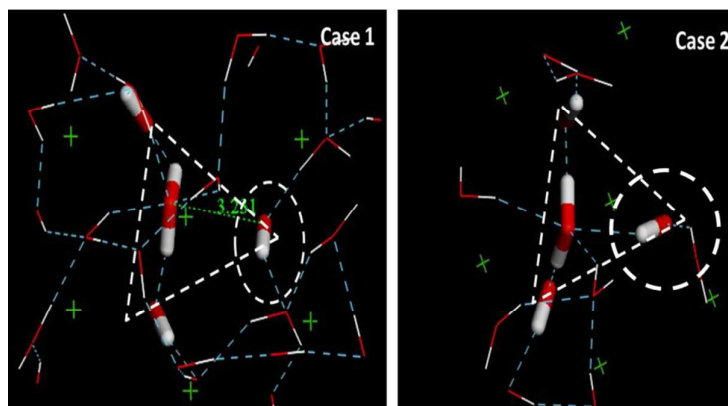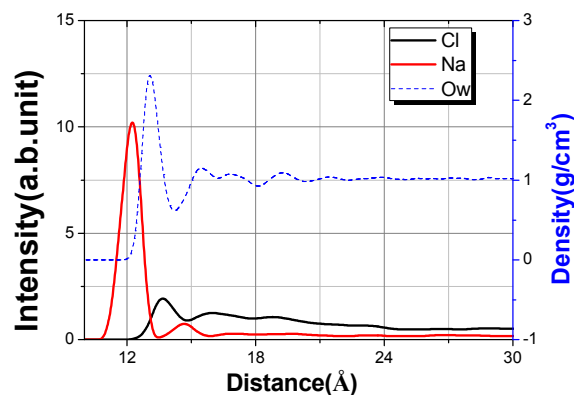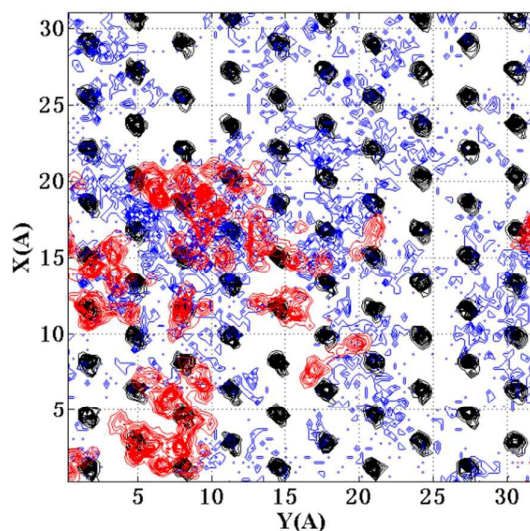

Fig: 10 the neighboring oxygen atoms for type 3 water molecules

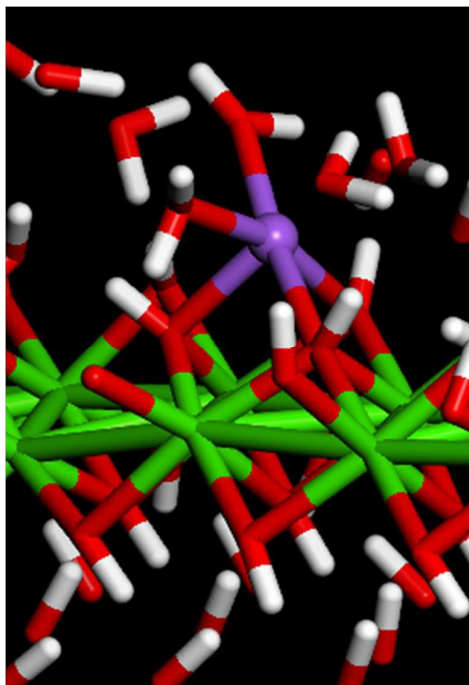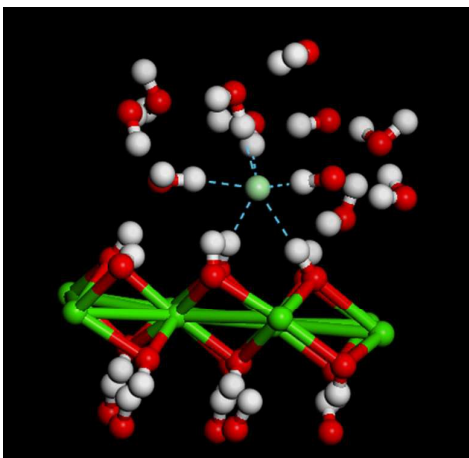**3.3 Ions adsorption on the surface**

(a)

(b)

Fig. 11 (a) atomic density profiles for Cl and Na ions of portlandite-water interface;
 (b) Contour maps for the Na (red) and Cl ions (blue) near the surface

5 Na and Cl ions were added into the previous 1200 water molecules system to simulate a 0.2mol/L NaCl solution interaction with portlandite surface, in a 35 Å pore. A 10ns simulation time was used to give a more statistical reliable result. As shown in Fig. 11a, the peaks for the Cl and Na ions near the surface indicate the calcium hydroxyl groups prefer to adsorb both ions. Calculated from the density profiles for all the configurations, about 21.5% of Cl ions are bound to the surface within the 3 Å region and more than 92.7% sodium atoms form connections with the surface within the 3 Å distance. Experimentally, ^{35}Cl NMR relaxation methods (Yu & Kirkpatrick, 2001) investigated on the portlandite crystal in contact with sodium chloride solution. The experimental results showed that $Ca(OH)_2$ is capable of adsorbing chloride ions. The larger peaks of Na density profiles and more dense contours of Na trajectories shown in Fig. 11b, illustrate that sodium atoms are more likely to be adsorbed on the surface. A previous simulation (Murray, et al., 2010) also indicated that the sodium atoms have more retention time on the substrate. The vibration of the surface hydroxyl groups result in local negative and positive charge elements in the portlandite surface that lead to the adsorption of Na and Cl ions respectively. As

shown in Fig. 12 a, when the nearest 4 hydroxyl neighbors tilt opposite to each other, the exposed surface oxygen atoms result in a negative charge; on the other hand, as exhibited in Fig. 12 b, if the nearest 4 hydroxyls point toward each other, it results in a local positive region. The former case can attract Na atoms, while the latter case is suitable for Cl adsorption. Because of the smaller size of the sodium ions (radius less than 2.35 Å), they easily penetrate into the vacancies between the substrate hydroxyls and develop bonding between Na and O. Therefore, the geometrical constraint for the sodium ions makes sodium atoms vibrate in the surface. Deeper penetration can further screen the influence from the surface water and other ions; therefore the relative stable connection between the surface hydroxyl and sodium ions allows the ions to remain for a long time. Compared with sodium ions, the chloride ions with large atom radii can only diffuse near the surface, with 2 H-bonds formation between the OH and Cl⁻. The adsorbed chloride ions, only one side being influenced by the substrate hydroxyls, are enclosed by the water molecules. Rapid formation and breakage of the H-bonding leads to rapid adsorption and desorption. The adsorption state on the surface of different ions can result in large discrepancies between the different ions in the respect of dynamic properties, which is discussed in the following part.

(a)

(b)
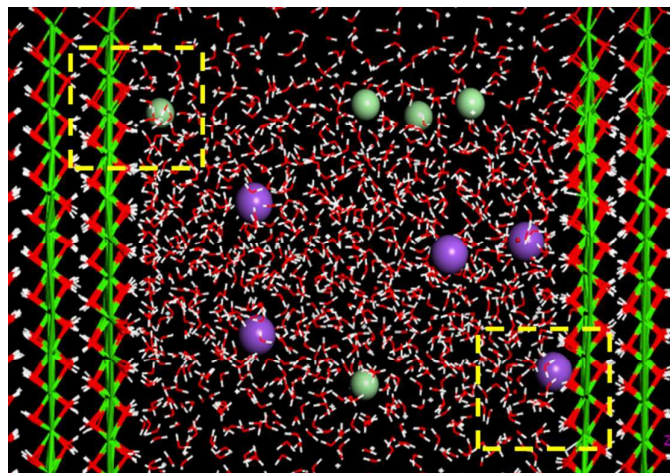
(c)

Fig.12 snapshots for the ions adsorption on portlandite surface

3.4 Dynamic behaviors of water and ions

The diffusion coefficient, a parameter to estimate the dynamic properties of water molecules, is achieved from the mean squared displacement (MSD) by the following equation 4.

$$2Dt = \frac{1}{n} < |r_i(t) - r_i(0)|^2 > \tag{4}$$

In the equation, $r_i(t)$ represents the position of atom i at time t and n is the dimension of the calculated diffusion coefficient. There are three diffusion coefficients considered in our simulation: D_{xyz}, the bulk diffusion coefficient, that is taken into account in the coordinates in 3 directions (n=3); D_{xy}, only considering the diffusion in direction parallel to the substrate (n=2); D_z, reflecting the diffusion normal to the surface (n=1). The positions of the water molecules are determined by the coordinates of oxygen atoms from the equilibrium configuration, every 0.1 ps. The MD trajectories are divided into 10ps trajectories, andeach recorded configuration is used as the origin of a new 10ps trajectory. The interlayer water region is divided into several layers parallel to the surface. The Diffusion coefficient is calculated for each individual layer. For a typical 1ns simulation, each layer coefficient is obtained from 10000 10-ps configurations (Kerisit & Liu, 2009). The layer width is about 2 Å.

As shown in Fig. 13a, the three obvious peak in the O_w atomic density distribution indicates an adsorption layer of nearly 1nm. This transitional water layer between the bulk water solution and the portlandite substrate is highly influenced by the charge and the geometry of interface structures. Due to the interface adsorption effect and the constraint from ordered surface hydrogen bonding, water molecules near the surface slabs have less probability to exchange with water in other slabs, the constrained displacement leads to the lower diffusion coefficient in interfacial zone. Only when the water moves more than 1.5nm from the surface, the water diffusion coefficient approximates to the value in bulk water. The diffusion coefficient can be decomposed into x, y and z directions to further detect the influence on the interfacial region. In Fig. 13a, the discrepancy between D_{xy} and D_z indicate water movements perpendicular to the surface are more constrained compared with movement parallel dimension. Near the second peak around 5 Å and the third peak around 7.5 Å, the curve has no obvious increase because the high density of water also reduces velocity. With progressively increasing distance from the surface, the diffusion coefficient continues to increase until 15 Å from the surface. Even though the density profile shows no large fluctuation 10 Å away, the influence on the dynamic properties can extend to an even longer region. In addition, since no channel water exists, as in the jennite-water and tobermorite-water interface, the transformation is from surface state to the bulk solution state in a relative moderate mode.
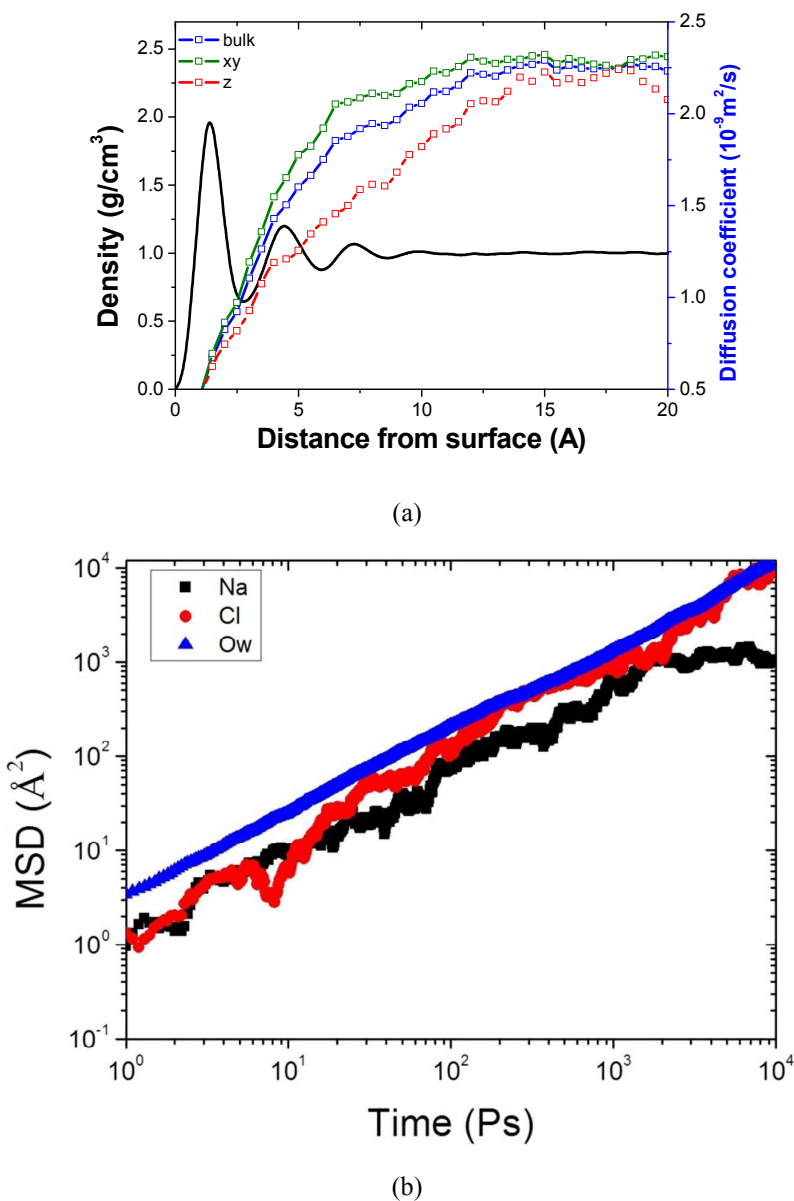
(a)

(b)

Fig. 13 (a) diffusion coefficient of water molecules evolution with distance away from the portlandite surface; (b) mean square displacement changes with time for the water molecules, chloride ions and sodium ions.

Based on the MSD curves exhibited in Fig. 13b, the bulk diffusion coefficients of chloride ions, sodium ions and water molecules are 1.78×10^{-9}, 0.12×10^{-9} and 2×10^{-9} m^2/s. It should be noted that the mobility for sodium ions is dramatically smaller than that of chloride ions. It means that the hydroxyl surface significantly

slows down the movement of sodium ions. The large discrepancy can be understood from the previous molecular structural analysis. The sodium ions penetrating into the calcium hydroxyl groups are strongly restricted in the structural cage and can remain near the surface for a long time. The surficial sodium ions, with a slow diffusion rate, are quite similar to those interlayer molecules ultra-confined in the nanopores of C-S-H gel that show a glassy dynamic nature with a long caging region (Youssef, et al., 2011).
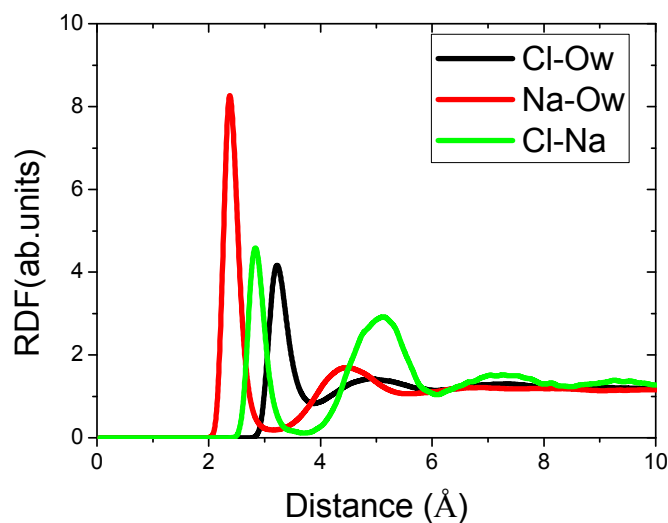
(a)
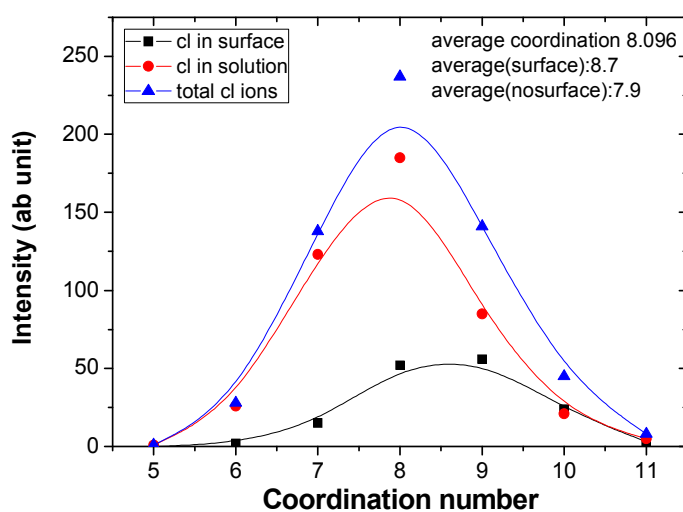
(b)
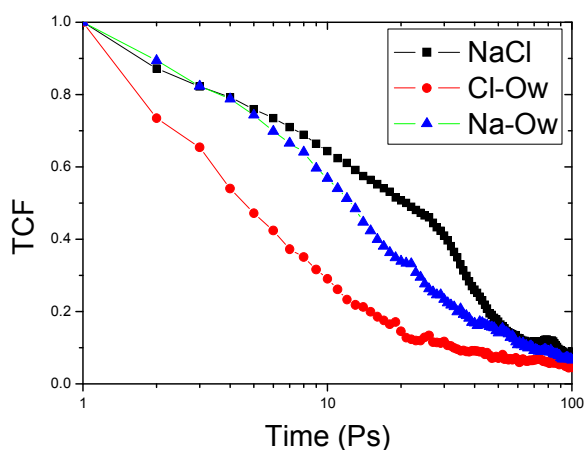
(c)

Fig.14 (a) Radial distribution function for Na-O$_w$, Cl-O$_w$ and NaCl (b) coordination

number distribution for Cl in surface and Cl in pore solution; (c) time correlated

function for Na-Cl pair, Cl-O$_w$ cluster, Na water cluster and Cl-H bonds

The local structure of an electrolyte solution can be conveniently studied by means of

ion–ion, ion–water, and water–water pair correlation or the radial distribution

functions. It can be observed in Fig. 14a that there are two pronounced peaks at 2.83

Å and 5.13 Å for the RDF of Na-Cl. The spatial correlation at 2.83 Å indicates the

contact for sodium and chloride ions and the maximum at 5.13 Å corresponds to the

solvent separating ions in the solution. The contact ions pair and solvent separated

ions have also been found in KCl solution in previous research, which can be taken as

structural characteristic for ions in the electrolyte solution (Chowdhuri & Chandra,

2001). In Fig. 14a, it also presents the ion–water pair correlation functions for NaCl

solution. The average hydration number of water molecules in the first shell of

sodium ions and chloride ions are 5.46 and 8.1, respectively. These numbers are

obtained by integrating the ion–oxygen pair correlation functions up to the first

minimum. It should be pointed out that the hydration number of the chloride ions is

slight higher than that in the bulk NaCl solution obtained in previous experiments and

simulation (7.5~8) (Uchida & Matsuoka, 2004). Fig. 14b demonstrates the

coordination number distribution for the chloride ions diffusing in the pore solution

and those near the surface. On average, ions near the interface region have 0.8 more coordinated atoms than those in pore solution, which is attributed to the dense H-bonds formation between Cl⁻ and hydroxyl groups.

The time correlated function (TCF) is utilized to describe dynamical properties of ions-water and ions-ions correlations. TCF of pairs in the NaCl solution is represented in Eq(5):

$$C(t) = \frac{<\delta b(t)\delta b(0)>}{<\delta b(0)\delta b(0)>} \tag{5}$$

where $\delta b(t) = b(t)-< b >$, b(t) is a binary operator that takes a value of one if an ion–water pair is within the nearest neighbor separation (in the hydration shell) at time t and zero otherwise, and <b> is the average value of b over all simulation time and pairs. The border of the hydration shell is defined as the first minimum of ion–oxygen RDF which is shown in Fig.14a. The physical meaning of *C(t)* is the probability that a water molecule or ion, which was in the hydration shell of ion i initially, is also in the hydration shell of the same at time t. The time correlated functions for ions-water and ions-ions are exhibited in Fig.14c. The decay of *C(t)* describes the dynamics of ion–water pair structural relaxation and its relaxation time τ can be obtained by integrating the *C(t)* function:

$$\tau_{res} = \int_0^\infty C_\theta(t)\, dt \tag{6}$$

The residence time can be interpreted as the time a water molecule spends on average in the vicinity of an ion. The calculated residence time for different pairs is listed in the following order: τNaCl (28.88ps) > τNa-O_w (22.83ps) > τCl-O_w (13.15ps). The longer residence time can be attributed to the more stable chemical connections. The sequence for the lifetime of ions-water pairs matches well with previous investigation of ions in the bulk solution without influence of calcium hydroxyl surface. In general,

the residence time of a water molecule near a sodium ion is much longer compared to that near potassium or chloride ions. The sodium ions, having smaller ionic radium, show stronger ion-water connection in compared with the Cl-O$_w$ pair. Interestingly, the long lifetime of Na-Cl connections implies the strong strength of chemical bond between positive and negative ions in the electrolyte solution. The NaCl cluster formation, slowing down the mobility for both ions, has also been found in C-S-H gel pore solution simulation in previous research (Hou & Li, 2014). It should be noted that the presence of calcium hydroxyl extends of the residence time for the ions-water pairs. Chowdhuri and Chandra (Chowdhuri & Chandra, 2001) investigated the dynamics for the ions-water cluster in the bulk electrolyte solution with concentration less than 0.5 mol/L and obtained the lifetimes for the Na and Cl ions of 18.5 ps and 10 ps, respectively, which are shorter than those for ions confined in the portlandite. The lifetime enhancement can be interpreted by two reasons: the two-dimensional confining geometry imposed by the substrate restricts the mobility of ions along z direction; the surficial hydroxyl groups supplies a great number of donate sites for the H-bonds between Cl and water and negative oxygen site for the Na-O connections.

4. Conclusions

Molecular dynamics was employed to investigate the atomic structure and dynamics of the water and ions transport in the vicinity of calcium hydroxyl surface and conclusions have been made as follows:

1. On the (001) surface of portlandite, water molecules diffusing near the calcium hydroxyl surface demonstrate special features dramatically different from those in bulk water solution: large density, good orientation preference, ordered interfacial organization and low diffusion rate.

2. The surface water molecules have more H-bonds connection and coordination oxygen atoms both from the neighboring water molecules and solid surface. Due to different H-bonds contribution, three types of surface water molecules featured by the dipolar angle distribution were distinguished. Water molecules within the

first adsorbed layer about 2 Å from the hydroxyl surface tend to adopt H-downward distribution as they donate H-bonds to oxygen in the solid surface. On the contrary, the H-upward preference was observed as water molecules accept H-bonds from neighboring hydrogen in portlandite.

3. With increasing distance from channel, the structural and dynamical behavior of water molecules vary and gradually translate into bulk water properties at 10~15 Å from liquid-solid interface.

4. The diffusion coefficients of water molecules and ions in the vicinity of portlandite surface are slowed down due to geometrical and electrical restrictions from solid hydroxyl groups. The Na^+ ions, deeply rooted in the vacancy region of surficial hydroxyl groups, are significantly slowed down and remain near the surface with long time. On the other hand, the weak H-bonds forming by the chloride ions and hydroxyl cannot restrict the adsorbed chloride ions for longer time.

5. When the water and ions are confined in the nano-pores, the residence time for the ions-water, ions-ions cluster is elongated so that the ions adsorption capability for porlandite surface is enhanced due to the stable Na-Cl connections in the electrolyte solution.

Acknowledgement

Reference

Bordallo, H. N., Aldridge, L. P. & Desmedt, A., 2006. Water dynamics in hardened ordinary portland cement paste or concrete: from quasielastic neutron scattering. *Journal of Physics and Chemistry B 110,* pp. 17966-17976.

Castellote, M., Andrade, A. & Alonso, C., 1999. Chloride-binding isotherms in concrete submitted to non-steady-state migration experiments. *Cement and Concrete Research,* Volume 29, pp. 1799-1806.

Chowdhuri, S. & Chandra, A., 2001. Molecular dynamics simulations of aqueous NaCl and KCl solutions: Effects of ions concentration on the single particle, pair and collective dynamic properties of ions and water molecules. *Journal of Chemical Physics,* 115(8), pp. 3732-3741.

Cygan, R. T., Greathouse, J. A., Heinz, H. & Kalinichev, A. G., 2009. Molecular models and simulations of layered materials. (Invited). *Journal of Materials Chemistry, 19,* pp. 2470-2481.

Cygan, R. T., Liang, J. J. & Kalinichev, A. G., 2004. Molecular models of hydroxide, oxyhydroxide, and clay phases and the development of a general force field. *Journal of Physical Chemistry, 108,* pp. 1255-1266.

Delagrave, A. et al., 1998. Chloride binding capacity of various hydrated cement paste systems. *Advanced in Cement Based Materials,* Volume 6, pp. 28-35.

Desgranges, L. et al., 1993. Hydrogen thermal motion in calium hydroxide: Ca(OH)2. *Acta Crystallographica Section B: Structural Science,* 49(5), pp. 812-817.

Greener, J. et al., 2000. Monitoring of hydration of white cement paste with proton NMR spin–spin relaxation. *Journal of the American Ceramic Society,* 83(3), pp. 623-627.

Holuj, F., Drozdowski, M. & Czajkowski, M., 1985. Brillouin Spectrum of Ca(OH)2. *Solid State Communications,* 56(12), pp. 1019-1021.

Hou, D. & Li, Z., 2014. Molecular dynamics study of water and ions transport in nano-pore of layered structure: A case study of tobermorite. *Microporous and Mesoporous Materials,* Volume 195, pp. 9-20.

Hou, D., Zhao, T., Ma, H. & Li, Z., 2015. Reactive Molecular Simulation on Water Confined in the Nanopores of the Calcium Silicate Hydrate Gel: Structure, Reactivity, and Mechanical Properties. *The Journal of Physical Chemistry C,* 119(3), pp. 1346-1358.

Kalinichev, A. G. & Kirkpatrick, R. J., 2002. Molecular Dynamics Modeling of Chloride Binding to the Surfaces of Calcium Hydroxide, Hydrated Calcium Aluminate, and Calcium Silicate Phases. ,. *Chemistry of Materials,* 14(8), pp. 3539-3549.

Kalinichev, A. G., Wang, J. & Kirkpatrick, R. J., 2007. Molecular dynamics modeling of the structure, dynamics and energetics of mineral water interfaces: application to cement materials.. *Cement and Concrete Research, 37,* pp. 337-347.

Kerisit, S. & Liu, C. X., 2009. Molecular simulation of water and ion diffusion in nanosized mineral fractures. *Environ. Sci. Technol, 43,* pp. 777-782.

Kirkpatrick, R. J., Kalinichev, A. G. & Wang, J., 2005. Molecular dynamics modeling of mineral interlayers and surfaces: Structure and dynamics. *Mineralogical Magazine, 69,* pp. 287-306.

Kirkpatrick, R. J. et al., 2005. Molecular modeling of the vibrational spectra of interlayer and surface species of layered double hydroxides. In: The Application of Vibrational Spectroscopy to Clay Minerals and Layered. *The Clay Mineral Society, Aurora, CO. CMS Workshop Lecture Series, 13,* pp. 239-285.

Korb, J. P., Monteilhet, L., McDonald, P. J. & Mitchell, J., 2007. Microstructure and texture of hydrated cement-based materials: A proton field cycling relaxometry approach. *Cement and concrete research,* 37(3), pp. 295-302.

Laugesen, J., 2005. Density functional calculations of elastic properties of portlandite, Ca(OH)2. *Cement and Concrete Research,* 35(2), pp. 199-202.

Murray, S. J., Subramani, V. J., Selvam, R. P. & Hall, K. D., 2010. Molecular Dynamics to Understand the Mechanical Behavior of cement Paste. *Journal of the transportation Research Board, 2142,* pp. 75-82.

Plimpton, S., Thompson, A., Crozier, P. & Kohlmeyer, A., 2001. *LAMMPS Molecular Dynamics Simulator.* [Online]

Available at: http://lammps.sandia.gov/index.html

[Accessed 18 January 2014].

Templeton, J. et al., 2011. A Long-Range Electric Field Solver for Molecular Dynamics Based on Atomistic-to-Continuum Modelling. *Journal of Chemical Theory and Computation,* 7(6), pp. 1736-1749.

Uchida, H. & Matsuoka, M., 2004. Molecular dynamics simulation of solution structure and dynamics of aqueous sodium chloride solutions from dilute to supersaturated concentration. *Fluid Phase Equilibria,* 219(1), pp. 49-54.

Wang, J. W., Kalinichev, A. G. & Kirkpatrick, R. J., 2004. Molecular modeling of water structure in nano-pores between brucite (001) surfaces. ,. *Geochimica et Cosmochimica Acta,68,* pp. 3351-3365.

Youssef, M., Pellenq, R. J. M. & Yildiz, B., 2011. Glassy nature of water in an ultraconfining disordered material: the case of calcium− silicate− hydrate. *Journal of the American Chemical Society,* 133(8), pp. 2499-2510.

Yu, P. & Kirkpatrick, R. J., 2001. 35Cl NMR relaxation study of cement hydrate suspensions. *Cement and Concrete Research,* 31(10), p. 1479—1485.